Silicon High-Order Coupled-Microring-Based Electro-Optical Switches for On-Chip Optical Interconnects

Xianshu Luo, Junfeng Song, Shaoqi Feng, *Student Member, IEEE*, Andrew W. Poon, *Member, IEEE*, Tsung-Yang Liow, *Member, IEEE*, Mingbin Yu, Guo-Qiang Lo, *Member, IEEE*, and Dim-Lee Kwong, *Fellow, IEEE*

Abstract—We demonstrate an electro-optically (EO) tunable switch using tenth-order coupled-microring resonators in silicon-on-insulator using complementary metal–oxide–semiconductor fabrication technology. The measured drop-port transmission spectra show box-like transmission passband with ∼100-GHz bandwidth and ∼50-dB extinction ratio. With a DC voltage supply to the integrated p-i-n diodes surrounding the microrings, the optical switch shows, respectively, ∼10 and ∼45-dB on/off ratios from throughput- and drop-port. The measured EO switching times are ∼1 ns upon a 1.2-Vpp low-speed driving signal and a DC power consumption of ∼37 mW. Up to 30-Gb/s pseudorandom binary sequence ($2^{31} - 1$) signal transmissions suggest high-data-rate signal switching capability.

Index Terms—Coupled resonators, electrooptic devices, integrated optoelectronics, ring resonator, silicon-on-insulator technology.

I. INTRODUCTION

IN next-generation high-bandwidth low-power computing systems, the conventional on-chip copper interconnect becomes bandwidth-limiting and also causes excessive electrical power consumption [1]. Silicon-based on-chip optical interconnects [1, 2], where high-bandwidth optical signals are routed through integrated low-loss optical waveguides, is recognized as one of the promising alternatives due to the key merits of large bandwidth, low power consumption and compatibility with complementary metal-oxide-semiconductor (CMOS) process. In last few years, various high-performance optical components required for on-chip optical interconnects

using silicon or hybrid-silicon materials have been demonstrated. Microring resonators, as one of the key building blocks for silicon photonics [2–6], are used extensively for optical switches due to the wavelength selectivity and the relatively low power consumption. However, single microring resonator-based optical switches only display Lorentzian-shaped response, thus limit the bandwidth and the crosstalk performance [2]. In order to attain large-bandwidth and high-extinction-ratio optical switches, high-order coupled-microring structures have been proposed and demonstrated [2–4, 6]. While many demonstrations of high-order coupled-microrings structures focused on the passive device design for enhanced filtering performance [7], high-speed reconfigurable switches [3–6] are required for photonic integration.

In this letter, we demonstrate an electro-optically (EO) tunable switch using 10th-order coupled-microring resonators. The adoption of the high-order microring structure leads to the box-like flat-top transmission passband with ∼100 GHz bandwidth and ∼ 50 dB extinction ratio. The EO switch on/off ratio is ∼ 10 dB and ∼ 45 dB for throughput and drop transmissions, respectively. The switching times are ∼ 1 ns with the DC power consumption of ∼ 37 mW. High-performance signal transmissions are demonstrated using up to 30 Gbit/s pseudorandom binary sequence (PRBS) signals.

II. DESIGN AND FABRICATION

We fabricate the lateral p-i-n diode integrated 10th-order coupled-microring resonators in silicon-on-insulator (SOI) by using CMOS-compatible fabrication process. The SOI wafer is with a 220 nm silicon layer sitting on a 3 μm buried oxide (BOX) layer. The device is patterned by using deep ultra-violet (DUV) photolithography, followed by a two-step silicon reactive ion etching (RIE) to form a rib waveguide for ion implantation and a channel waveguide for the nano-taper. The slab thickness is ∼ 60 nm. The p-i-n diodes which only surround the microring arc regions (excluding the coupling regions) are formed by ion implantation in the slab layer. A ∼ 2 μm oxide is deposited as an upper cladding, followed by contact holes opening. Finally, aluminum is deposited and patterned to form the contact pads.

Fig. 1(a) shows the optical microscope image of the fabricated switch. The white lines illustrate the waveguides underneath. The microrings are identically designed with 10 μm
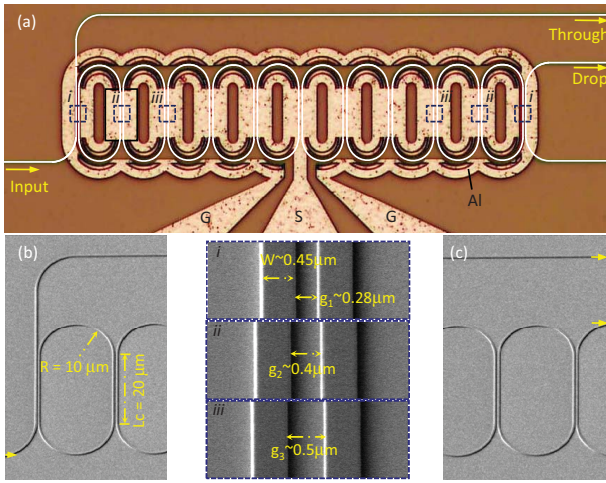
Fig. 1. (a) Optical microscope image of the fabricated tenth-order coupled-microring-based switch integrated with lateral p-i-n diodes. (b) and (c) Zoomed-in SEMs of the input and output coupling regions. Insets: Zoomed-in SEMs of (i) waveguide-microring coupling region and (ii), (iii) inter-microring coupling regions. G: ground. S: signal. Al: aluminum.

radii and 20 μm coupling lengths. In this fabrication run, all the 10 p-i-n diodes of the 10 microrings are connected together for the ease of EO tuning. We expect that all microring resonances identically blue-shift in wavelength when forward-biasing the p-i-n diodes. Figs. 1(b) and (c) show the zoom-in scanning-electron micrographs (SEMs) of the input and output coupling regions. In order to achieve box-like filter response with flat-top, broad transmission band and steep roll-off, yet without significant passband intensity fluctuation, the apodization design [8] is adopted with varied gap separations. The insets (i)-(iii) show the SEMs of the coupling gaps. The waveguide width is $\sim$ 450 nm for the side-coupled waveguides and the microring waveguides. The gap spacings are symmetrically designed with mirror symmetry around the center gap. The gap spacing between the input (output) waveguide and the first (last) microring is $\sim$ 280 nm. The gap spacing between the first (10th) and second (9th) microrings is $\sim$ 400 nm. All the rest of the gaps are designed identically of $\sim$ 500 nm.

III. RESULTS AND ANALYSIS

Fig. 2(a) shows the measured throughput and drop transmission spectra without voltage supply. The transmission spectra are normalized to the fiber-to-fiber transmission. Thus, the insertion losses include the input/output coupling losses and the propagation loss. The free-spectral range (FSR) is $\sim$ 6 nm ($\sim$ 750 GHz). In the spectral range of 1530 nm to 1598 nm, there are total 11 optical transmission bands, which suggest high-throughput multi-channel parallel data switching and transmission [3]. For the drop-port, all the channels display $\sim$ 50 dB extinction ratio (ER). For the throughput-port, the highest ER is only $\sim$ 10 dB, which is attributed to the fabrication imperfection induced resonance wavelength misalignment. It is possible to increase the throughput ER by some trimming processes or dynamic control of each microring.

The optical switching between throughput- and drop-port is realized according to free-carrier dispersion effect by
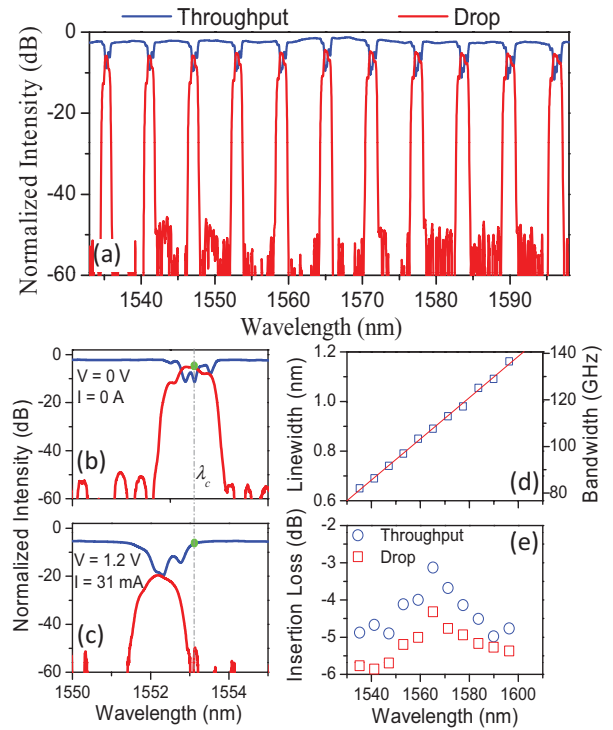

Fig. 2. (a) Measured TE-polarized throughput and drop transmission spectra with $\sim$50-dB extinction ratio from the drop-port. Demonstration of the electro-optical tunable switching with (b) $V = 0$ V, $I = 0$ A, and (c) $V = 1.2$ V, $I = 31$ mA at 1553.1 nm. The switch-on/off ratio is, respectively, $\sim$10 and $\sim$45 dB in the throughput and drop. λ_c: carrier wavelength. Measured (d) linewidths and (e) throughput/drop loss distributions for all the 11 optical channels.
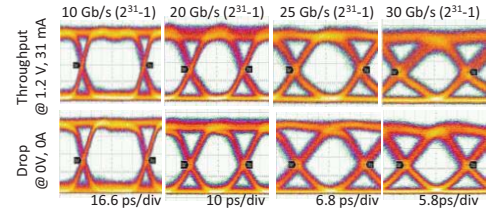

Fig. 3. Eye diagrams of the transmitted 10, 20, 25, and 30-Gb/s PRBS signals ($2^{31} - 1$) from the throughput- and drop-ports.

supplying DC voltages to the p-i-n diodes. Fig. 2(b) shows the zoom-in view of the throughput and drop transmission spectra at $\sim$1553 nm with no bias, which clearly shows the box-like passband with sharp roll-off and $\sim$ 50dB extinction ratio. The 3-dB linewidth is $\sim$ 0.8 nm ($\sim$100 GHz). At carrier wavelength λ_c of $\sim$1553.1 nm aligning to the passband center, the insertion losses are $\sim$ -15 dB and $\sim$ -5.2dB for throughput and drop, suggesting signal transmission to the drop-port at this state, with $\sim$ 10 dB crosstalk. From the throughput transmission, we only observe four resonance dips, which suggest possible fabrication imperfection-induced resonance wavelength misalignment. In order to compensate such misalignment, dynamic tuning of each microring is required. When supplying a 1.2V DC voltage to the p-i-n diodes (Fig. 2(c)), the transmission band blueshifts with the drop-port intensity significantly reduce due to the free-carrier absorption loss. The transmission intensities at the
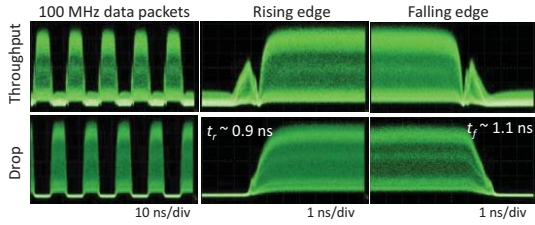
Fig. 4.   Measured dynamic responses of the EO switch from the throughput- and drop-ports by switching 20-Gb/s signals. The data packets are 100-MHz square wave with 1.2 Vpp and 50% duty cycle.

TABLE I
PERFORMANCE METRICS OF THE TENTH-ORDER
COUPLED-MICRORING SWITCH

Bandwidth (GHz)	ER (dB)	FSR (nm)	Total insertion loss (dB)		t_r/t_f (ns)	Switch Power (mW)
			Throughput	Drop		
80-140	50	6	3.1-4.9	4.3-5.9	0.9/1.1	37

carrier wavelength are ~ -4.1 dB for the throughput-port and ~ -50 dB for the drop-port, suggesting signal transmission to the throughput, with ignorable cross talk. Thus, the on/off ratios for the throughput and drop are ~ 10 dB and ~ 45 dB. The DC power consumption according to the current-voltage measurement is ~ 37 mW. We mention that the relatively high free-carrier absorption loss (~ 15 dB) and power consumption (~ 37 mW) is due to the large wavelength blueshift (~ 1 nm) for all 10 microrings in order to obtain sufficient on/off ratio in the throughput transmission.

We summarize the passband linewidth and the total insertion losses for all the 11 optical channels, as shown in Fig. 2(d) and (e). The linewidth linearly increases from ~ 0.6 nm (80 GHz) to ~ 1.2 nm (140 GHz), which is attributed to the increased inter-cavity coupling with wavelength. The throughput and drop insertion losses are defined as the throughput and drop intensity at the carrier wavelength with and without DC voltage supply (green dots in Fig. 2(b), (c)). The throughput losses range from 3.1 dB to 4.9 dB, while the drop losses range from 4.3 dB to 5.9 dB, suggesting the intensity non-uniformity of ~ 1.6 dB.

In order to investigate the signal transmission, we send 10/20/25/30-Gbit/s PRBS signals (bit length 2^{31}-1) to the optical switch and measure the transmitted signals from both throughput- and drop-ports. The carrier wavelength is 1553.1 nm. For the throughput transmission measurement, we supply a 1.2V forward-bias to the p-i-n diodes. Fig. 3 shows the measured eye diagrams from the throughput- and drop-ports. The open eye diagrams suggest the high-quality data switching and transmission. For all the measured eye diagrams, the ERs are exceeding 12 dB while the peak-to-peak jitters are ~ 10 ps. We have confirmed the signal transmission through all 11 channels, which all show similar performances.

We measure the dynamic performances of the optical switch by sending a 20 Gbit/s data stream to the switch while EO modulating it by a 100 MHz square wave with 1.2 Vpp and 50% duty cycle. Fig. 4 shows the measured dynamic responses of the optical switches. We observe ~ 0.9 ns and 1.1 ns 10%-90% rising and 90%-10% falling times from the drop-port, which are limited by the carrier injection and diffusion. We attribute the small peaks in the rising and falling edges of the throughput response to the mode-splitting-induced multiple dips in the throughput transmission (See Fig. 2(b), (c)). The number of peaks depends on the choice of the carrier wave-length. Such small peaks can be minimized by optimizing the apodization design in order to flatten the throughput resonance dips. We also find peaks with much smaller amplitudes from the drop-port transmission, due to the nearly flat-top drop-port transmission (See Fig. 2(b), (c)). However, we see no significant signal distortion effects from such small peaks to both the throughput and drop signals (See Fig. 3).

Table I summarizes the performances of the demonstrated switch.

IV. CONCLUSION

We have demonstrated an electro-optically tunable switch by using 10th-order coupled-microring resonators in SOI. We show a periodic transmission bands with 6 nm free-spectral range, ~ 100 GHz bandwidth and ~ 50dB drop-port extinction ratio. The on/off ratio are respectively ~ 10 dB and 45 dB in throughput and drop, with ~ 1 ns switching time and 37 mW DC power consumption. High-quality 30-Gbit/s PRBS signal ($2^{31} - 1$) transmission with open eye diagrams suggests high-data-rate signal switching capability. Such wideband, high extinction ratio and high switching-speed optical switches are applicable for next-generation high-performance on-chip optical interconnects.

REFERENCES

[1] D. Miller, "Device requirements for optical interconnects to silicon chips," *Proc. IEEE*, vol. 97, no. 7, pp. 1166–1185, Jul. 2009.

[2] A. W. Poon, X. Luo, F. Xu, and H. Chen, "Cascaded microresonator-based matrix switch for silicon on-chip optical interconnection," *Proc. IEEE*, vol. 97, no. 7, pp. 1216–1238, Jul. 2009.

[3] Y. Vlasov, W. M. J. Green, and F. Xia, "High-throughput silicon nanophotonic wavelength-insensitive switch for on-chip optical networks," *Nature Photon.*, vol. 2, pp. 242–246, Mar. 2008.

[4] M. S. Dahlem, C. W. Holzwarth, A. Khilo, F. X. Kärtner, H. I. Smith, and E. P. Ippen, "Reconfigurable multi-channel second-order silicon microring-resonator filterbanks for on-chip WDM systems," *Opt. Express*, vol. 19, no. 1, pp. 306–316, Jan. 2011.

[5] H. L. R. Lira, S. Manipatruni, and M. Lipson, "Broadband hitless silicon electro-optic switch for on-chip optical networks," *Opt. Express*, vol. 17, no. 25, pp. 22271–22280, 2009.

[6] A. Biberman, *et al.*, "Broadband silicon photonic electrooptic switch for photonic interconnection networks," *IEEE Photon. Technol. Lett.*, vol. 23, no. 8, pp. 504–506, Apr. 15, 2011.

[7] S. Xiao, M. H. Khan, H. Shen, and M. Qi, "A highly compact third-order silicon microring add-drop filter with a very large free spectral range, a flat passband and a low delay dispersion," *Opt. Express*, vol. 15, no. 22, pp. 14765–14771, 2007.

[8] P. Chak and J. E. Sipe, "Minimizing finite-size effects in artificial resonance tunneling structures," *Opt. Lett.*, vol. 31, no. 17, pp. 2568–2570, 2006.